Review of Scientific Instruments

Apparatus for simultaneous dynamic light scattering–small angle neutron scattering investigations of dynamics and structure in soft matter

Cite as: Rev. Sci. Instrum. **92**, 023907 (2021); https://doi.org/10.1063/5.0035529
Submitted: 29 October 2020 • Accepted: 14 January 2021 • Published Online: 12 February 2021

V. Nigro, R. Angelini, S. King, et al.

AIP Publishing

Review of Scientific Instruments ARTICLE scitation.org/journal/rsi

Apparatus for simultaneous dynamic light scattering–small angle neutron scattering investigations of dynamics and structure in soft matter

Cite as: Rev. Sci. Instrum. 92, 023907 (2021); doi: 10.1063/5.0035529
Submitted: 29 October 2020 • Accepted: 14 January 2021 •
Published Online: 12 February 2021

V. Nigro,[1,a] R. Angelini,[1,2,b] S. King,[3] S. Franco,[4,1] E. Buratti,[1] F. Bomboi,[1] N. Mahmoudi,[3] F. Corvasce,[1,c] R. Scaccia,[1,c] A. Church,[3] T. Charleston,[3] and B. Ruzicka[1,2,b]

AFFILIATIONS

[1] Institute for Complex Systems, National Research Council (CNR-ISC), Sapienza University of Rome, Pz.le A. Moro 2, 00185 Rome, Italy
[2] Department of Physics, Sapienza University of Rome, Pz.le A. Moro 2, 00185 Rome, Italy
[3] ISIS Pulsed Neutron and Muon Source, STFC Rutherford Appleton Laboratory, Harwell Campus, Didcot, Oxon OX11 0QX, United Kingdom
[4] Dipartimento di Scienze di Base e Applicate per l'Ingegneria (SBAI), Sapienza University of Rome, 00185 Rome, Italy

[a] **Present address:** ENEA C.R. Frascati, FSN-TECFIS-MNF Photonics Micro and Nanostructures Laboratory, Via E. Fermi 45, 00044 Frascati, Rome, Italy.
[b] **Authors to whom correspondence should be addressed:** roberta.angelini@cnr.it and barbara.ruzicka@cnr.it
[c] **Present address:** Institute of Structure of Matter, National Research Council (CNR-ISM) Via del Fosso del Cavaliere 100, I-00133 Rome, Italy.

ABSTRACT

Dynamic Light Scattering (DLS) and Small-Angle Neutron Scattering (SANS) are two key tools to probe the dynamic and static structure factors, respectively, in soft matter. Usually, DLS and SANS measurements are performed separately, in different laboratories, on different samples, and at different times. However, this methodology has particular disadvantages for a large variety of soft materials, which exhibit a high sensitivity to small changes in fundamental parameters, such as waiting times, concentration, pH, and ionic strength. Here, we report on a new portable DLS-SANS apparatus that allows one to simultaneously measure both the microscopic dynamics (through DLS) and the static structure (through SANS) on the same sample. The apparatus has been constructed as a collaboration between two laboratories, each an expert in one of the scattering methods, and was commissioned on the *LOQ* and *ZOOM* SANS instruments at the ISIS Pulsed Neutron and Muon Source, U.K.

I. INTRODUCTION

Soft materials are ubiquitous in a variety of industries, including foods, pharmaceuticals, personal care products, and cosmetics. They exhibit unique behaviors that are often fundamental to their applications in those industries[1] but which stem from their microscopic properties.[2,3] Soft materials also offer the possibility to investigate many of the key topics in soft condensed matter in general, such as slow reactions and kinetics, aging processes, gelation, controlled release, food processing, micellar growth, and aggregation phenomena. Correlating the microscopic behavior with these macroscopic processes is thus a fertile ground for research.

Light scattering has long been used for the characterization of soft matter and dynamic light scattering (DLS) has demonstrated itself to be a crucial and indispensable technique to investigate the dynamics.[4] DLS measures the stochastic temporal variations in the scattered laser light, resulting in a time autocorrelation function describing the timescales of mutual diffusive motion of the scattering objects. This information can then be used to derive the hydrodynamic size of objects in suspension.[5,6] However, the autocorrelation

function itself is especially useful for investigating the microscopic dynamics of soft matter systems, including colloids,[7–9] polymers,[10] microgels,[11,12] proteins,[13] and vesicles,[14] and for characterizing phenomena such as sol–gel transitions[15] or the formation of arrested states through changing concentration or waiting time (aging).[16–18] All this is possible because the technique studies spatial perturbations of the order of a micrometer or less (a typical scattering vector is of the order of $Q = 10^{-2}\,\mathrm{nm}^{-1}$) but also probes time scales in the range of nanoseconds and above. These two conditions typically characterize a wide range of soft matter systems.

Techniques such as (Ultra-)Small-Angle Scattering, whether performed with x-rays [(U)SAXS] or neutrons [(U)SANS], are capable of probing soft matter on comparable to somewhat complementary length scales as light scattering, typically from a few nm to hundreds of nm.[19–21] However, compared to DLS, these techniques are only capable of studying the time-averaged structure in the system. The best laboratory SAXS or SANS instruments might achieve a time resolution of around 100 ms in an optimal system (although sub-millisecond time resolution has been demonstrated with a rare form of SANS called TISANE[22]), while even synchrotron SAXS would be hard-pressed to achieve better than 100 μs. On the other hand, the great advantage of neutrons is that they permit one to selectively highlight, or suppress, the scattering from one or more components in a complex soft matter system by deuteration. This "contrast variation" approach is possible with light and x-rays (by varying the refractive index or electron density, respectively) but, in practical terms, is extremely difficult to execute. There is, therefore, a clear scientific benefit to performing simultaneous DLS-SANS measurements on soft matter systems arising from the synergy between the two techniques. The clear disadvantage of SANS, of course, is that (at present) it can only be performed at large-scale facilities.

Today, the use of multiple experimental techniques is recognized to be of fundamental importance to understanding the properties of real-world materials. In particular, combining information about both structural and dynamical behavior is imperative since it is the complex interplay between the structure and dynamics that determines the microscopic relaxation processes responsible for the macroscopic mechanical properties of a material. This knowledge is crucial for a detailed understanding of properties of samples and to facilitate the tailored design of materials with specific properties.[23,24] Within this framework, reliably performing simultaneous DLS and SANS measurements would represent a breakthrough in helping develop our understanding of this underlying and often complex behavior that simply cannot be uniquely determined through the use of a single technique.

Given the above, it will not be a surprise to learn that combining DLS with SAXS/SANS has been a goal of several groups in recent years. Kohlbrecher *et al.*[25] augmented a high-pressure SANS sample environment with a DLS. Nawroth *et al.*[26] and later Heigl *et al.*[27] both combined DLS with stop-flow SANS. Schwamberger *et al.*[28] implemented DLS-SAXS on a flow-through capillary for online metrology purposes, while Falke *et al.*[29] designed a multichannel DLS system for the BioSAXS endstation at PETRA III. However, because the vast majority of soft matter SANS experiments are conducted on fluid samples in cuvettes, which are both optically and neutronically transparent, delivering a capability for DLS-SANS with a sample changer has remained a key aspiration of the SANS community.

The aim of the present paper is to report on a new compact portable DLS apparatus, conceived, designed, and implemented by a team from the Institute for Complex Systems (ISC), CNR, Italy, working in collaboration with SANS scientists and engineers from the ISIS Pulsed Neutron and Muon Source, UK. The apparatus is fully enclosed to meet stringent safety regulations, has a relatively small footprint, and includes a temperature-controlled sample changer. When installed on a SANS instrument, the apparatus permits complementary and simultaneous information on the microscopic structure (through SANS) and dynamics (through DLS) of soft matter systems to be acquired. In this paper, we validate the performance of the instrument by performing simultaneous DLS and SANS measurements on dilute polymer nanoparticle samples and compare the radii derived through the two techniques.

II. DESIGN CRITERIA

While SAXS/SANS instruments are often highly adaptable to the sample environment needs of an experiment, equipment complexity and experimental turnaround time are generally divergent quantities. This becomes an important consideration at large-scale facilities where the inherent cost of beam time is high and there is an ethos of minimizing downtime. Laser safety is another important consideration in these multi-user working environments. While laser hazards can always be mitigated by engineered controls and interlocks, if these are infrastructural, as distinct from local to the apparatus, then the portability of the apparatus is sacrificed.

With these considerations in mind, the new apparatus has been designed to satisfy several competing requirements: an enclosed "drop in"/"modular" apparatus with a compact footprint, sufficiently robust to facilitate use on any of the four SANS instruments at ISIS (or, in principle, elsewhere), with its own interlock system, easy to align (both neutronically and optically) in a reproducible manner, and incorporating a temperature-controlled sample changer (to reduce operator interaction with the laser, to make more efficient the use of neutron beamtime, and indeed to facilitate useful science).

From the outset, one of the most challenging aspects of the design was the need to maintain as minimal an air path for the neutrons as possible. This was because the "cold" neutrons used in SANS are significantly attenuated and scattered by the much more massive gas molecules in air. As evacuating the apparatus was not considered a practical solution, given most soft matter samples are fluids, this meant that the feasibility of the design depended on one important technological challenge: namely, miniaturizing the optical elements of the apparatus sufficiently while retaining good quality optical data. Achieving this would naturally also help make the apparatus compact and portable.

To find out, a simple prototype DLS apparatus was constructed at the CNR-ISC in order to experiment with different optical geometries and beam paths. The efficiency of these setups was then characterized in terms of the quality of the autocorrelation function acquired in a given time from a polystyrene latex dispersion standard using the same sort of sample cuvette and sample volume (≈250 μl) as would be used for a SANS experiment.

From combining the design criteria with the prototyping, we then arrived at the final setup shown in Fig. 1. A "lift-on/lift-off"

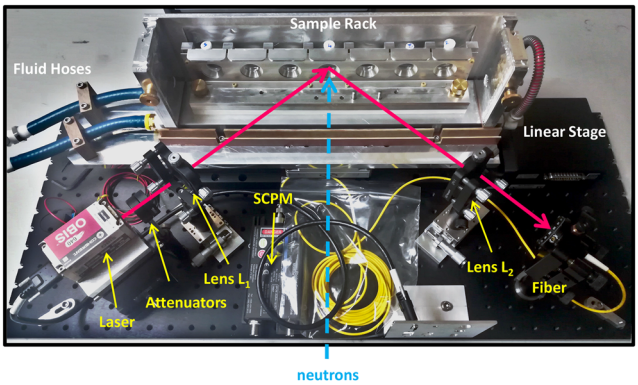

FIG. 1. Photograph of the DLS-SANS apparatus without the enclosure. The cover of the sample rack assembly, which aids temperature control, is also removed for clarity. The red arrows indicate the path of the laser beam, while the dashed cyan arrow indicates the path of the neutron beam.

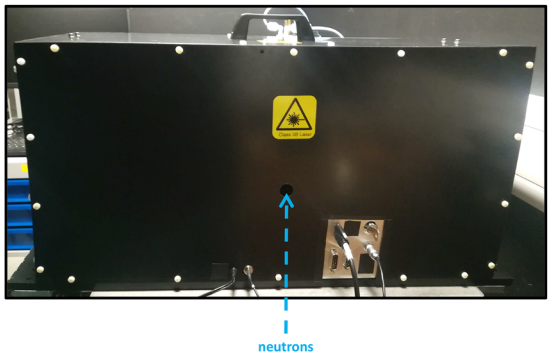

FIG. 2. Photograph of the DLS-SANS enclosure. The dashed cyan arrow indicates the path of the neutron beam. The aperture shown for the incoming neutron beam is 20 mm in diameter.

interlocked enclosure, presenting a robust physical boundary capable of adequately containing the laser radiation generated within it, protects operators on the outside and helps exclude dust and facilitate temperature control.

III. APPARATUS DESCRIPTION

The DLS-SANS apparatus (see Fig. 1) comprises a black anodized aluminum optical breadboard (780 × 350 × 13 mm^3, Thorlabs) onto which all of the system is mounted. The output from a solid state laser of 100 mW power at λ = 642 nm (Coherent® OBIS 640 LX) is attenuated through an interchangeable optical filter and focused onto the center of a sample cuvette (1 mm or 2 mm pathlength, e.g., Hellma GmbH Type 120-QS or Starna Scientific Type 32-Q) through the lens L_1. A short linear translation stage (M-ILS250PP, Newport Instruments) permits movement of a temperature-controlled sample changer assembly on which is mounted a seven-position rack (in-house design, ISIS Pulsed Neutron and Muon Source) that houses the sample cuvettes. Temperature control is achieved using an external circulating fluid bath and monitored with thermocouples on the sample rack.

The laser beam scattered from the sample is then collected by the lens L_2 and directed on to a single mode fiber feeding a Single-Photon Counting Module (SPCM-AQRH-13-FC, PerkinElmer). The resulting electrical signal is then passed to an LSi logarithmic correlator[30] that computes the intensity autocorrelation function.

The optical elements (Thorlabs) are mounted on micrometers that permit horizontal (H) and vertical (V) translations and tilt (T) and focus (F) movements to facilitate alignment. In particular, the following movements are allowed: laser (H, V), lens (H, V, T, F), and fiber (H, V, T). The scattering angle is $\theta_1 = 105^\circ$, which, according to the relation $Q = |\vec{Q}| = (4\pi n/\lambda)\sin(\theta/2)$, where n is the index of refraction (note $n = 1$ for neutrons), corresponds to a scattering vector $Q = 0.021$ nm^{-1} for aqueous samples.

A rigid black plastic enclosure (350 mm high), but with an aluminum back wall, fits over and locates on the breadboard, completely enclosing everything inside (see Fig. 2). The only apertures in the cover are for the passage of the neutron beam (also these are normally covered by aluminum foil to preserve light-tightness), a cut-out on the left side where the fluid hoses emanate from, and a cut-out on the front wall permitting access to a connector panel. Neither of the last two apertures exposes the direct or reflected laser beam. There are no optical windows on the enclosure. The aperture in the back cover for the outgoing neutron beam subtends an angle of ±40° relative to the axis of the neutron beam. This is sufficient to illuminate all the low- and high-angle detectors in use on the ISIS SANS instruments in their normal operational configurations. The reason for an aluminum back wall, behind the samples, is that some neutrons will be scattered by the sample to large angles and ultimately pass through the back wall instead of through the foil-covered neutron beam exit window. If these were to subsequently reach the neutron detector, they would contaminate the SANS from the sample. Neutronically, there is much less SANS from aluminum than from plastic. An alternative strategy would be to simply glue 1 mm thick cadmium sheet (a neutron absorber) onto the aluminum back wall. However, the use of cadmium introduces an additional hazard.

The presence of the enclosure and its lid engages microswitches that form part of the laser interlock system. For sample changes, undoing six thumbscrews allows just the lid of the enclosure to be removed, but this operation breaks the laser interlock. For optical alignment of the apparatus, a key switch on the front connector panel (visible in Fig. 2) allows suitably authorized persons to operate the laser without the lid, or indeed the enclosure, in place. The DLS apparatus is optically aligned for the measurements before it is placed on the beamline. For such an alignment, the cover is removed, a cuvette is filled with a calibration standard, and the intensity of the DLS signal is maximized by slightly changing the vertical, horizontal, and tilt movements of the fiber and the vertical and horizontal movements of lens L_1 and lens L_2 in an iterative procedure. Once the intercept and shape of the intensity autocorrelation function $g_2(Q, t)$ and the derived particle size confirm the goodness of the alignment, all the movements are locked and the cover is replaced. The alignment is then re-checked after installation on the beamline by remeasuring the calibration standard. As long as the apparatus has been handled carefully, alignment is usually maintained.

The overall dimensions of the apparatus are 780 × 350 × 363 mm^3 (length × width × height), and its total mass is about 30 Kg.

IV. EXPERIMENTAL METHODS

The apparatus has so far been used on both the *LOQ* and *ZOOM* SANS instruments at ISIS with excellent performance. Photographs of the apparatus installed on the *LOQ* and on the *ZOOM* instruments are shown in Figs. 3(A) and 3(B), respectively. In the following, we report DLS-SANS data obtained on the *LOQ* instrument.

A. SANS measurements

SANS measurements were performed on the *LOQ* instrument located on Target Station 1 at the ISIS Pulsed Neutron and Muon Source (STFC Rutherford Appleton Laboratory, Didcot, U.K)[31] This is a time-of-flight diffractometer with a typical time-averaged flux at the sample of 3 × 10^5 cm^{-2} s^{-1} at 25 Hz, which utilizes a polychromatic incident neutron beam spanning wavelengths of $0.22 \leq \lambda \leq 1.0$ nm, simultaneously recorded on two, two-dimensional "area" detectors with overlapping angular coverage, to provide a very wide dynamic range in scattering vector of $0.07 \leq Q \leq 14$ nm^{-1} but with fixed sample–detector distances of 0.5 m and 4.1 m. This type of SANS instrument is ideal for studies where the length scales of interest are uncertain, or broad, or indeed evolving, as time-consuming instrumental re-configurations and re-calibrations are unnecessary. The neutron beam incident on the sample was collimated to 8 mm in diameter.

Using the Mantid framework (version 4.1.0),[32] each raw SANS dataset was corrected for the incident neutron wavelength distribution, the detector efficiency, spatial linearity, the measured sample transmission, and the sample path length before being radially averaged and converted into the coherent elastic differential scattering cross section $[\partial\Sigma/\partial\Omega(Q)]$ as a function of Q, hereafter simply referred to as intensity, $I(Q)$. This process also merged the data from the two detectors onto a common Q scale. The contribution from instrumental (vacuum windows, etc.) and sample (cuvette, incoherent scattering, etc.) background scattering was removed by subtracting the SANS measured from a pure D_2O sample. Finally, the fully reduced SANS data were placed on an absolute intensity scale by reference to the scattering from a partially deuterated solid polystyrene blend standard sample of known molecular weight, measured with the same instrument configuration.[33] SANS data analysis was performed using the Sasview software.[34]

B. DLS-SANS measurements

To test the performance of the DLS-SANS apparatus, measurements were first made on a light scattering standard sample of known size, then subsequently on a colloidal suspension of microgel particles of contemporary interest.

It is worth mentioning that in order to use the DLS-SANS apparatus, one has to verify that the samples under investigation are not turbid to avoid multiple scattering of the photons. At the moment, the use of cross correlation techniques[35,36] is, in fact, precluded due to space limitations. Since SANS is an inherently count rate limited technique, this means increasing the SANS measurement time to compensate for the use of dilute samples. In our testing, we did explore some of this envelope. The lowest concentration we measured was a microgel sample at C_w = 0.03%, but obviously, the size of the particles being studied and their refractive index had a bearing on this. The LOQ instrument is, by modern standards, a relatively low flux instrument. On the ZOOM instrument, we were able to effectively halve counting times. For testing the DLS-SANS apparatus, samples were investigated at a very low concentration to ensure that the particles were non-interacting so that the hydrodynamic radii could be confidently obtained from DLS and compared with the radii derived from the SANS form factor.

1. Standard sample

An aqueous polystyrene latex standard (PLS; Nanosphere™ 3000 Series, Fisher Scientific UK) was diluted with D_2O from 1% solids to a weight concentration of C_w = 0.06%. The latex spheres were certified as having a nominal radius of (31 ± 3) nm.

Representative examples of the resulting DLS intensity autocorrelation functions, $g_2(Q,t) - 1$, are shown in Fig. 4(A) and those of the SANS data, $I(Q)$, in Fig. 4(B). The SANS data were acquired over 9 h. The DLS data were measured for 120 s but repeated 17 times with a delay of 1800 s between repetitions. Hence, during a single SANS measurement, many DLS correlation functions were acquired.

The particle size was then extracted from the intensity autocorrelation function by fitting it to the conventional Kohlrausch–William–Watts (KWW) expression,[37–39]

$$g_2(Q,t) = 1 + b(A^{-(t/\tau)^{\beta}})^2, \quad (1)$$

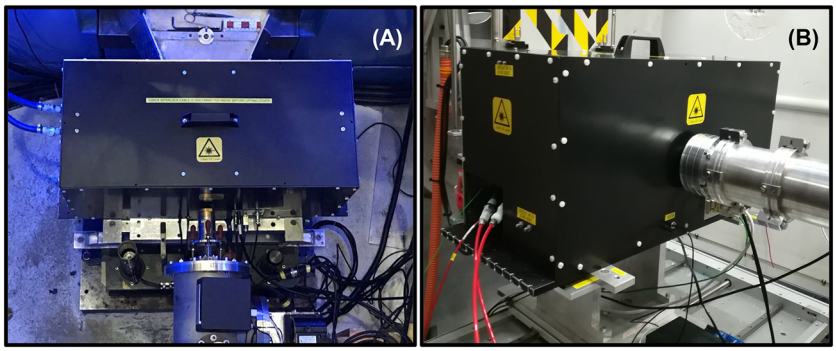

FIG. 3. Photographs of the DLS-SANS apparatus installed on the (A) LOQ and (B) ZOOM SANS instruments at ISIS. The neutron beam emanates from the silver-colored pipes in each image.

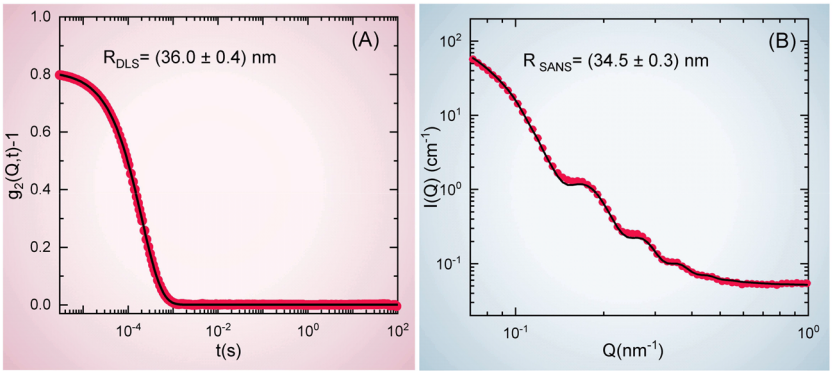

FIG. 4. (A) Intensity autocorrelation function and (B) SANS intensity as simultaneously obtained from the PLS sample using the DLS-SANS apparatus. The continuous black lines superimposed on the data (symbols) are fits to Eqs. (1) and (3), respectively.

where τ is the relaxation time and β describes the deviation from the simple exponential decay ($\beta = 1$), which gives a measure of the distribution of relaxation times. In this case, a value of $\beta \cong 1$ was found as expected given the low size polydispersity (PD) of the standard sample. Alternatives to Eq. (1), such as Cumulant analysis or the Contin algorithm, can be successfully employed for the determination of the average particle size and width of the particle size distribution, even if some limitations may result from a lack of robustness when dealing with more complex systems.

The diffusion coefficient D was then derived from τ using the relation $\tau = 1/DQ^2$, and from that, the hydrodynamic radius of the particles was estimated using the Stokes–Einstein relationship for spherical particles,

$$R = \frac{k_B T}{6\pi\eta D}, \tag{2}$$

where k_B is the Boltzmann constant, T is the sample temperature (T = 295 K for these measurements), and η is the solvent viscosity (η = 0.9544 mPa at T = 295 K[40]). From this analysis, a value of R_{DLS} = (36.0 ± 0.4) nm was obtained.

The SANS from non-interacting monodisperse spherical particles of uniform scattering length density (SLD) is given by[41]

$$I(Q) = \Phi V(\Delta\rho)^2 \left[\frac{3(\sin(QR) - QR\cos(QR))}{(QR)^3}\right]^2 + bkgd, \tag{3}$$

where Φ is the volume fraction of particles, V is the volume of one particle, $\Delta\rho$ is the difference in neutron scattering length density (SLD[42]) between the particles (ρ_{PSL} = +1.42 × 10^{10} cm^{-2}) and the dispersion medium (ρ_{H2O} = −0.56 × 10^{10} cm^{-2} and ρ_{D2O} = +6.33 × 10^{10} cm^{-2}), R is the radius of the particles, and *bkgd* is the residual Q-independent background. Where necessary, Eq. (3) can be integrated over a particle size distribution. Here, polydispersity was not taken into account, assuming a highly monodisperse sample, but the estimated dQ data were used for instrumental resolution smearing.

Least-squares fitting Eq. (3) to the SANS data returned a value of R_{SANS} = (34.5 ± 0.3) nm in very good agreement with the expected radius and with R_{DLS}. This gave confidence that the DLS-SANS apparatus was working as intended. Note that it is not uncommon for $R_{DLS} > R_{SANS}$ as the former typically includes a "shell" of coordinated solvent molecules that moves with the particle and retards Brownian diffusion. The difference observed here is entirely consistent with measurements of the typical thickness of this solvent shell.[43]

2. PNIPAM microgel sample

The second sample that has been investigated was an aqueous suspension of poly(N-isopropylacrylamide) (PNIPAM) microgel particles. PNIPAM microgels are thermoresponsive colloidal particles having rather different dimensions on either side of a temperature-induced Volume Phase Transition (VPT). The particles collapse from a swollen to a shrunken state at T ≅ 305 K. This soft colloid, and its derivatives, has been widely studied in the literature both from the fundamental science perspective and for its many potentially innovative applications.[44–46] For the present study, a PNIPAM microgel was synthesized in our laboratory following the procedure fully described in Refs. 47 and 48. A dispersion of the microgel in D_2O at a weight concentration C_w = 0.3% was measured at T = 293 K, below the VPT, and at T = 313 K, above the VPT. Representative examples of the resulting DLS intensity autocorrelation functions, $g_2(Q,t) - 1$, are shown in Fig. 5(A) and those of the SANS data, $I(Q)$, in Fig. 5(B). The SANS data were acquired over 8 h at T = 20 °C and over 6.5 h at T = 40 °C. The DLS data at T = 20 °C were acquired with 25 repetitions of 120 s and at T = 40 °C with 20 repetitions of 120 s, with intervals of 1000 s between repetitions. Hence, again, during a single SANS measurement, a large number of DLS correlation functions were obtained. Thus, through the DLS data, it is therefore possible to monitor any changes in the behavior of the sample that are occurring during each SANS measurement. However, in the future work, we expect to be able to correlate the DLS data with time-sliced SANS data.

The differences between the swollen and shrunken states are clearly evident in both cases. As before, the DLS data have been fitted to Eqs. (1) and (2) to obtain the hydrodynamic sizes of the microgel particles. This yielded R_{DLS} = (34.4 ± 1.2) nm at T = 293 K and R_{DLS} = (20.3 ± 1.4) nm at T = 313 K.

Interpreting these SANS data is, however, a little more complicated because, unlike the standard sample, the internal structure of the microgel particles is not homogeneous and the interface with the dispersion medium is less-defined. The former condition can be accounted for by assuming that the distance between cross-links in the microgel (the "mesh size") can be described by a single density correlation length. The scattering from this is the well-known Ornstein–Zernicke model, which has a Lorenztian form. The second condition can be accounted for by taking the scattering function for a sphere [the term in the square brackets in Eq. (3)] and convoluting

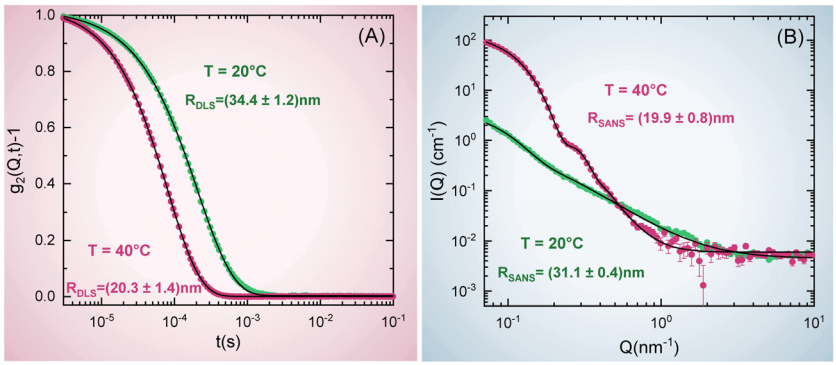

FIG. 5. (A) Normalized intensity autocorrelation function and (B) SANS intensity as simultaneously obtained from the PNIPAM microgel sample at T = 293 K (below the VPT) and at T = 313 K (above the VPT) using the DLS-SANS apparatus. The continuous black lines superimposed on the data (symbols) are fits to Eqs. (1) and (4), respectively.

it with a decay function to "soften" the drop-off in scattering length density at the periphery of the sphere. A common decay function that is applied is a Gaussian, and this leads to a model known as the "fuzzy sphere."[49] The overall scattering function is then a sum of the two contributions:[50,51]

$$I(Q) = \left[\frac{\Phi}{V}\left[\frac{3V\Delta\rho(\sin(QR) - QR\cos(QR))}{(QR)^3}\ \exp\left(\frac{-(\sigma Q)^2}{2}\right)\right]^2 + \left[\frac{I_L(0)}{1+(\xi Q)^2}\right]\right] + bkgd, \quad (4)$$

where Φ, V, and $\Delta\rho$ all have the same meaning as before (with the scattering length density of PNIPAM $\rho_{PNIPAM} = +8.14 \times 10^9\ \mathrm{cm}^{-2}$). The parameter σ is the "fuzziness" of the particle interface, related to the distance over which the SLD decays from its starting value ($\sigma \ll R$). The way that this is defined means that in this model R is the radius at which the SLD profile has decreased by half. The overall radius of the microgel particle is then given by $R_{SANS} = R + 2\sigma$.[52] The gel structure itself is characterized by the correlation length ξ. $I_L(0)$ is the intensity of the Lorentzian contribution at Q = 0. Where necessary, Eq. (4) can be integrated over a particle size distribution. Radius polydispersity (PD) was accounted for with a Schulz distribution and the estimated dQ data were once again used to account for instrumental resolution smearing.

Least-squares fitting Eq. (4) to the SANS data returned values of R_{SANS} = (31.1 ± 0.4) nm with PD = 0.25 at T = 293 K and R_{SANS} = (19.9 ± 0.8) nm with PD = 0.14 at T = 313 K. These values are again in very good agreement with the hydrodynamic radii from the DLS. It is interesting to note that agreement is better when the microgel particles are in the shrunken state presumably because they then appear more homogeneous.

V. CONCLUSION

In this work, we have presented a new dynamic light scattering apparatus conceived to permit simultaneous DLS and SANS measurements and demonstrated that it produces good quality and reliable data with test measurements on two different samples (a polystyrene latex calibration standard and a poly(N-isopropylacrylamide) microgel dispersion) on two SANS instruments at the ISIS Pulsed Neutron and Muon Source. Using the DLS data to derive size information produced results in excellent agreement with the values obtained from the SANS data. However, the real benefit of DLS is its ability to provide information about the microscopic dynamical behavior in soft matter samples, particularly in those that are sensitive to small changes in physicochemical stimuli. This will be the focus of future work.

AUTHORS' CONTRIBUTIONS

B.R., R.A., and S.K. conceived the idea and the scheme of the apparatus. F.C. and R.S. provided the technical design and mechanically realized the apparatus that was assembled by F.B. A.C. and T.C. provided the sample changer and technical assistance during the SANS experiments. V.N. did the alignment. V.N., R.A., E.B., S.F., and B.R. performed the measurements and the analysis with the help of S.K. and N.M. B.R., V.N., S.K., R.A., and N.M. wrote the manuscript. B.R. supervised the project.

Although commercial analysis software was provided with the correlator,[30] as part of this project, the KWW function [Eq. (1)] and Cumulant analysis functions were generated as plugin models for the SasView program. They are free to download from http://marketplace.sasview.org/.

ACKNOWLEDGMENTS

The authors thank Iain Johnson, Maksim Schastny, and Jamie Nutter (ISIS Sample Environment Electronics Team) and Alistair McGann, David Keymer, Thomas Willemsen, and John Holt (ISIS Instrument Control Software Team) for their assistance. This work was supported within the CNR-STFC Agreement 2014–2020 (Grant No. 3420) concerning collaboration in scientific research at the ISIS Spallation Neutron Source. The authors also gratefully acknowledge the UK Science and Technology Facilities Council for the provision of the neutron beam time at ISIS (Experiment Nos. RB1830612 http://doi.org/10.5286/ISIS.E.RB1830612-1, http://doi.org/10.5286/ISIS.E.RB1830612-2 and RB1920335 http://doi.org/10.5286/ISIS.E.RB1920355-1).

DATA AVAILABILITY

The data that support the findings of this study are available from the corresponding author upon reasonable request.

REFERENCES

[1] A. Fernandez-Nieves and A. Puertas, *Fluids, Colloids and Soft Materials: An Introduction to Soft Matter Physics* (John Wiley & Sons, 2016), pp. 1–432.
[2] R. Borsali and R. Pecora, *Soft-Matter Characterization* (Springer, 2008).
[3] C. N. Likos, "Effective interactions in soft condensed matter physics," Phys. Rep. **348**, 267–439 (2001).
[4] P. Pusey, "Introduction to scattering experiments," in *Neutrons, X-Rays and Light. Scattering Methods Applied to Soft Condensed Matter* (Elsevier Science B.V., 2002).
[5] M. Kaszuba, D. McKnight, M. T. Connah, F. K. McNeil-Watson, and U. Nobbmann, "Measuring sub nanometre sizes using dynamic light scattering," J. Nanopart. Res. **10**, 823–829 (2008).
[6] D. G. Dalgleish and F. R. Hallett, "Dynamic light scattering: Applications to food systems," Food Res. Int. **28**, 181–193 (1995).
[7] P. N. Pusey and W. van Megen, "Phase behaviour of concentrated suspensions of nearly hard colloidal spheres," Nature **320**, 340–342 (1986).
[8] K. N. Pham, A. M. Puertas, J. Bergenholtz, S. U. Egelhaaf, A. Moussaïd, P. N. Pusey, A. B. Schofield, M. E. Cates, M. Fuchs, and W. C. K. Poon, "Multiple glassy states in a simple model system," Science **296**, 104–106 (2002).
[9] T. Eckert and E. Bartsch, "Re-entrant glass transition in a colloid-polymer mixture with depletion attractions," Phys. Rev. Lett. **89**, 125701 (2002).
[10] W. Burchard and W. Richtering, "Relaxation in polymers," in *Dynamic Light Scattering From Polymer Solutions*, Progress in Colloid and Polymer Science (Steinkopff, 1989), pp. 151–163.
[11] V. Nigro, R. Angelini, B. Rosi, M. Bertoldo, E. Buratti, S. Casciardi, S. Sennato, and B. Ruzicka, "Study of network composition in interpenetrating polymer networks of poly(N isopropylacrylamide) microgels: The role of poly(acrylic acid)," J. Colloid Interface Sci. **545**, 210–219 (2019).
[12] V. Nigro, B. Ruzicka, B. Ruta, F. Zontone, M. Bertoldo, E. Buratti, and R. Angelini, "Relaxation dynamics, softness, and fragility of microgels with interpenetrated polymer networks," Macromolecules **53**, 1596–1603 (2020).
[13] Z. Yu, J. C. Reid, and Y.-P. Yang, "Utilizing dynamic light scattering as a process analytical technology for protein folding and aggregation monitoring in vaccine manufacturing," J. Pharm. Sci. **102**, 4284–4290 (2013).
[14] A. Grimaldi, C. Serpe, G. Chece, V. Nigro, A. Sarra, B. Ruzicka, M. Relucenti, G. Familiari, G. Ruocco, G. R. Pascucci, F. Guerrieri, C. Limatola, and M. Catalano, "Microglia-derived microvesicles affect microglia phenotype in glioma," Front. Cell. Neurosci. **13**, 41 (2019).
[15] M. Kroon, G. H. Wegdam, and R. Sprik, "Dynamic light scattering studies on the sol-gel transition of a suspension of anisotropic colloidal particles," Phys. Rev. E **54**, 6541–6550 (1996).
[16] A.-M. Philippe, D. Truzzolillo, J. Galvan-Myoshi, P. Dieudonné-George, V. Trappe, L. Berthier, and L. Cipelletti, "Glass transition of soft colloids," Phys. Rev. E **97**, 040601 (2018).
[17] W. van Megen and S. M. Underwood, "Glass transition in colloidal hard spheres: Mode-coupling theory analysis," Phys. Rev. Lett. **70**, 2766 (1993).
[18] B. Ruzicka, L. Zulian, and G. Ruocco, "Routes to gelation in a clay suspension," Phys. Rev. Lett. **93**, 258301 (2004).
[19] T. Zemb and P. Lindner, *Neutron, X-Rays and Light. Scattering Methods Applied to Soft Condensed Matter* (North Holland, 2002).
[20] I. Grillo, "Small-angle neutron scattering and applications in soft condensed matter," in *Soft Matter Characterization* (Springer, 2008), pp. 723–782.
[21] M. Monkenbusch and D. Richter, *Neutrons in Soft Matter* (John Wiley & Sons, 2011), pp. 147–182.
[22] C. Glinka, M. Bleuel, P. Tsai, D. Zákutná, D. Honecker, D. Dresen, F. Mees, and S. Disch, "Sub-millisecond time-resolved small-angle neutron scattering measurements at NIST," J. Appl. Crystallogr. **53**, 598–604 (2020).
[23] B. Ruzicka, E. Zaccarelli, L. Zulian, R. Angelini, M. Sztucki, A. Moussaïd, T. Narayanan, and F. Sciortino, "Observation of empty liquids and equilibrium gels in a colloidal clay," Nat. Mater. **10**, 56–60 (2011).
[24] R. Angelini, E. Zaccarelli, F. A. de Melo Marques, M. Sztucki, A. Fluerasu, G. Ruocco, and B. Ruzicka, "Glass-glass transition during aging of a colloidal clay," Nat. Commun. **5**, 4049–4057 (2014).
[25] J. Kohlbrecher, A. Bollhalder, R. Vavrin, and G. Meier, "A high pressure cell for small angle neutron scattering up to 500 MPa in combination with light scattering to investigate liquid samples," Rev. Sci. Instrum. **78**, 125101 (2007).
[26] T. Nawroth, P. Buch, K. Buch, P. Langguth, and R. Schweins, "Liposome formation from bile salt-lipid micelles in the digestion and drug delivery model $FaSSIF_{mod}$ estimated by combined time-resolved neutron and dynamic light scattering," Mol. Pharmaceutics **8**, 2162–2172 (2011).
[27] R. J. Heigl, M. Longo, J. Stellbrink, A. Radulescu, R. Schweins, and T. E. Schrader, "Crossover from a linear to a branched growth regime in the crystallization of lysozyme," Cryst. Growth Des. **18**, 1483–1494 (2018).
[28] A. Schwamberger, B. De Roo, D. Jacob, L. Dillemans, L. Bruegemann, J. W. Seo, and J. P. Locquet, "Combining SAXS and DLS for simultaneous measurements and time-resolved monitoring of nanoparticle synthesis," Nucl. Instrum. Methods Phys. Res., Sect. B **343**, 116–122 (2015).
[29] S. Falke, K. Dierks, C. Blanchet, M. Graewert, F. Cipriani, R. Meijers, D. Svergun, and C. Betzel, "Multi-channel *in situ* dynamic light scattering instrumentation enhancing biological small-angle X-ray scattering experiments at the PETRA III beamline P12," J. Synchrotron Radiat. **25**, 361–372 (2018).
[30] See https://lsinstruments.ch for information about the LSi logarithmic correlator used.
[31] R. K. Heenan, J. Penfold, and S. M. King, "SANS at pulsed neutron sources: Present and future prospects," J. Appl. Cryst. **30**, 1140–1147 (1997).
[32] Mantid: Manipulation and Analysis Toolkit for Instrument Data, version 4.1.0, 2013.
[33] G. D. Wignall and F. S. Bates, "Absolute calibration of small-angle neutron scattering data," J. Appl. Cryst. **20**, 28–40 (1987).
[34] See http://www.sasview.org/ for information about the SasView SANS analysis software.
[35] P. N. Pusey, "Suppression of multiple scattering by photon cross-correlation techniques," Curr. Opin. Colloid Interface Sci. **4**, 177–185 (1999).
[36] C. Urban and P. Schurtenberger, "Characterization of turbid colloidal suspensions using light scattering techniques combined with cross-correlation methods," J. Colloid Interface Sci. **207**, 150–158 (1998).
[37] R. Kohlrausch, "Theorie des elektrischen rckstandes in der leidener flasche," Ann. Phys. **167**, 179–214 (1854).
[38] G. Williams and D. C. Watts, "Non-symmetrical dielectric relaxation behaviour arising from a simple empirical decay function," Trans. Faraday Soc. **66**, 80–85 (1970).
[39] V. Nigro, R. Angelini, M. Bertoldo, F. Bruni, M. A. Ricci, and B. Ruzicka, "Dynamical behavior of microgels of interpenetrated polymer networks," Soft Matter **13**, 5185–5193 (2017).
[40] See https://wiki.anton-paar.com/en/water/ for a modern table of temperature-viscosity-density data for water.
[41] A. Guinier, G. Fournet, C. Walker, and K. Yudowitch, *Small-Angle Scattering of X-Rays*, Structure of Matter Series (John Wiley & Sons, 1955).
[42] See https://www.ncnr.nist.gov/resources/activation/ or https://sld-calculator.appspot.com/ for online neutron SLD calculators.
[43] S. L. J. Thomä, S. W. Krauss, M. Eckardt, P. Chater, and M. Zobel, "Atomic insight into hydration shells around facetted nanoparticles," Nat. Commun. **10**, 995 (2019).
[44] A. Fernandez-Nieves, H. Wyss, J. Mattsson, and D. Weitz, *Microgel Suspensions: Fundamentals and Applications* (Wiley-VCH Verlag, 2011).
[45] L. Rovigatti, N. Gnan, L. Tavagnacco, A. J. Moreno, and E. Zaccarelli, "Numerical modelling of non-ionic microgels: An overview," Soft Matter **15**, 1108–1119 (2019).
[46] J. Brijitta and P. Schurtenberger, "Responsive hydrogel colloids: Structure, interactions, phase behavior, and equilibrium and nonequilibrium transitions of microgel dispersions," Curr. Opin. Colloid Interface Sci. **40**, 87–103 (2019).
[47] V. Nigro, R. Angelini, M. Bertoldo, F. Bruni, M. Ricci, and B. Ruzicka, "Local structure of temperature and pH-sensitive colloidal microgels," J. Chem. Phys. **143**, 114904 (2015).

[48]V. Nigro, R. Angelini, M. Bertoldo, and B. Ruzicka, "Swelling of responsive-microgels: Experiments versus models," Colloids Surf., A **532**, 389–396 (2017).
[49]See https://www.sasview.org/docs/user/models/fuzzy_sphere.html for the SasView reference description of the fuzzy sphere model.
[50]P. S. Mohanty, D. Paloli, J. J. Crassous, E. Zaccarelli, and P. Schurtenberger, "Effective interactions between soft-repulsive colloids: Experiments, theory and simulations," J. Chem. Phys. **140**, 094901 (2014).
[51]A. Scotti, U. Gasser, E. S. Herman, M. Pelaez-Fernandez, J. Han, A. Menzel, L. A. Lyon, and A. Fernández-Nieves, "The role of ions in the self-healing behavior of soft particle suspensions," Proc. Natl. Acad. Sci. U. S. A. **113**, 5576–5581 (2016).
[52]M. Stieger, J. S. Pedersen, P. Lindner, and W. Richtering, "Are thermoresponsive microgels model systems for concentrated colloidal suspensions? A rheology and small-angle neutron scattering study," Langmuir **20**, 7283–7292 (2004).